

---

# SGLD-Based Information Criteria and the Over-Parameterized Regime

---

**Haobo Chen**  
University of Florida  
haobo.chen@ufl.edu

**Yuheng Bu**  
University of Florida  
buyuheng@ufl.edu

**Gregory W. Wornell**  
Massachusetts Institute of Technology  
gww@mit.edu

## Abstract

Double-descent refers to the unexpected drop in test loss of a learning algorithm beyond an interpolating threshold with over-parameterization, which is not predicted by information criteria in their classical forms due to the limitations in the standard asymptotic approach. We update these analyses using the information risk minimization framework and provide Akaike Information Criterion (AIC) and Bayesian Information Criterion (BIC) for models learned by stochastic gradient Langevin dynamics (SGLD). Notably, the AIC and BIC penalty terms for SGLD correspond to specific information measures, i.e., symmetrized KL information and KL divergence. We extend this information-theoretic analysis to over-parameterized models by characterizing the SGLD-based BIC for the random feature model in the regime where the number of parameters  $p$  and the number of samples  $n$  tend to infinity, with  $p/n$  fixed. Our experiments demonstrate that the refined SGLD-based BIC can track the double-descent curve, providing meaningful guidance for model selection and revealing new insights into the behavior of SGLD learning algorithms in the over-parameterized regime.

## 1 Introduction

The classical understanding of model selection is that more complex models can capture more complex patterns but tend to overfit and have large generalization error [1]. This tradeoff results in a U-shaped curve which is characterized by the classical model selection criterion when test loss is plotted against model complexity. As a result, the models that minimize test loss tend to have moderate complexity. Recently, the success of deep learning challenges this classical picture since neural networks are often extremely complex (e.g., able to fit random labels [2]) while *also* generalizing well to yield low test error on unseen samples.

An emerging explanation of this behavior is *double-descent* [3], which posits that: 1) The classical U-shaped curve is only valid when the number of model parameters  $p$  is smaller than the number of samples  $n$ . 2) In the over-parameterized regime where  $p$  is significantly larger than  $n$ , and models are complex enough to fit training data perfectly, test loss can decrease with increased model complexity.

To better understand the double-descent phenomenon, we revisit the classical derivations of information criteria and discern that the penalty term in Akaike Information Criterion (AIC) can be interpreted as the generalization error within a broader learning context, while Bayesian Information Criterion (BIC) approximates the marginal likelihood using the empirical risk minimization solution. We further update the classical analyses of AIC and BIC using the information risk minimization framework proposed in [4] by focusing on a specific stochastic algorithm—stochastic gradient Langevin dynamics (SGLD). It is shown in [5] that the generalization error achieved by SGLD can be characterized using information measures. This information-theoretic analysis motivates the proposed SGLD-based information criteria, which readily extend to over-parameterized models.

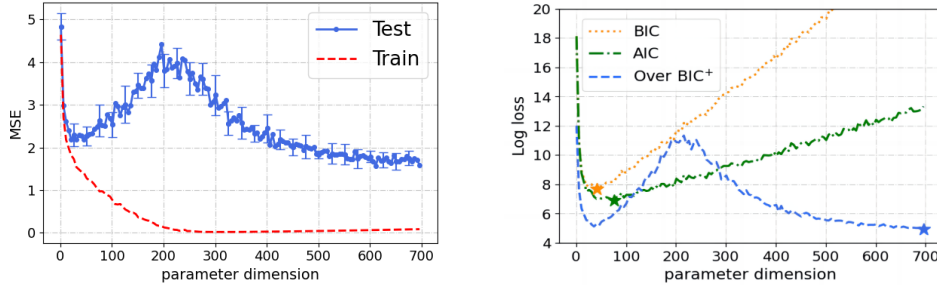


Figure 1: The test and training mean-squared error (MSE) (**left**) and the comparison of the proposed over-parameterized  $\text{BIC}^+$  with other classical information criteria (**right**) for over-parameterized RF models plotted with varying parameter dimension  $p$ . More details can be found in Section 5.2.

We make the following contributions in this paper:

1. We provide information-theoretic analyses for the generalization error and marginal likelihood of the model learned by the SGLD algorithm, resulting in SGLD-based AIC (equation (14)) and BIC (equation (17)) with different information measures as the penalty terms.
2. We show that the SGLD-based information criteria align with the classical information criteria in the classical large  $n$  regime theoretically (Theorem 1 and 2) and empirically (Section 5.1).
3. We generalize our information-theoretic analysis to over-parameterized random feature (RF) models, which results in an over-parameterized SGLD-based BIC (equation (27)) that effectively captures the double-descent behavior, which classical information criteria cannot; see Figure 1.
4. We empirically compare the SGLD-based BIC and AIC in the over-parameterized RF model by decomposing them into different terms (Section 5.2), where they favor different models similar to their classical counterparts. However, we observe that due to the differing impacts of the regularization (i.e., prior) in the over-parameterized regime, the double-descent behaviors of the AIC in population risk and that of the BIC in marginal likelihood can be quite complex.

**Related Work** Previous work has extended the classical BIC to high dimensions, e.g., [6, 7]. However, these works seek to *replace* maximizing marginal likelihood with a different criterion, substituting a penalty term  $pf(n)$  in place of the  $p \log n$  in BIC. By contrast, we retain the BIC criterion but analyze it beyond the classical regime for SGLD with an information-theoretic analysis.

Double-descent of the population risk with increasing model size was introduced in [3]; see also [8, 9]. An empirical demonstration of double-descent in modern deep networks is provided in [10]. A variety of work develops simplified models where the characterization of the double-descent curve can be obtained. For example, double-descent in linear regression models is investigated in [11, 12, 13, 14], and in linear classification models in [15, 16, 17]. The RF model has been adopted to understand double-descent in [18], which provides a generalization analysis of the performance achieved with ridge regression in the over-parameterized regime. In some of our analysis we likewise adopt this RF model [18, 19, 17, 20, 21], but with a different objective and analysis tools.

Double-descent phenomena have been explained from different perspectives. In [19, 22, 23], double-descent curves are explained via a refined version of bias-variance tradeoff, where the bias of the model decreases monotonically with the increase of  $p$ , but the variance increases and then decreases with  $p$ . And the connection of gradient descent dynamics and double-descent is discussed in [20, 8]. In [24, 25], sample-wise double-descent is studied under linear regression, and [26] shows that by adjusting the step sizes, sample-wise double-descent can be eliminated by early stopping.

Among recent work, our paper is most related to [27, 28], which also examines the difference between marginal likelihood and generalization error in model selection. However, by focusing on the SGLD, we are able to interpret the mismatch between AIC and BIC via information measures, which is more insightful in understanding double descent and other complex behaviors.

## 2 Preliminaries

We consider the following standard supervised learning problem formulation. Let  $S = \{Z_i\}_{i=1}^n$  be the training set, where each random sample  $Z_i = \{(X_i, Y_i)\} \in \mathcal{Z}$  are independent and identically distributed (i.i.d.) from the same data-generating distribution  $P_Z$ , and with the realization of this

sequence denoted as  $\mathbf{z}^n = (\mathbf{x}^n, y^n)$ . We denote the parameter of a machine learning model by  $w \in \mathcal{W}$ , where  $\mathcal{W}$  is the parameter space. The performance of the model is measured by a loss function  $\ell: \mathcal{W} \times \mathcal{Z} \rightarrow \mathbb{R}$ , and the log loss  $\ell_{\log}(w, \mathbf{z}) \triangleq -\log P(y|\mathbf{x}; w)$  associated with a parametric probabilistic model  $P(y|\mathbf{x}; w)$  is of particular interest to us.

We can define the empirical risk and the population risk associated with a given  $w$  as

$$L_E(w, \mathbf{z}^n) \triangleq \frac{1}{n} \sum_{i=1}^n \ell(w, \mathbf{z}_i), \quad L_P(w, P_Z) \triangleq \mathbb{E}_{P_Z} [\ell(w, Z)], \quad (1)$$

respectively. A learning algorithm can be modeled as a randomized mapping from the training set  $S$  onto a model parameter  $\hat{W} \in \mathcal{W}$  according to the conditional distribution  $P_{\hat{W}|S}$ .

Although the widely-used empirical risk minimization (ERM) is deterministic optimization, it is usually solved via stochastic gradient descent (SGD), which is random in nature. The ERM solution of log loss is the well-known maximum likelihood estimate (MLE), i.e.,  $\hat{W}_{\text{ML}} \triangleq \arg \max_w \hat{L}(w)$ , where  $\hat{L}(w) \triangleq \sum_{i=1}^n \log P_k(y_i|\mathbf{x}_i; w)$  denotes the log-likelihood on  $\mathbf{z}^n$ . The expected generalization error quantifying the degree of over-fitting can be expressed in the form

$$\overline{gen}(P_{\hat{W}|S}, P_S) \triangleq \mathbb{E}_{P_{\hat{W},S}} [L_P(\hat{W}, P_Z) - L_E(\hat{W}, S)], \quad (2)$$

where the expectation is taken over the joint distribution  $P_{\hat{W},S} = P_{\hat{W}|S} \otimes P_S$ .

## 2.1 The Classical Forms of AIC and BIC

The standard derivation of the AIC and the BIC arises from the classical asymptotic analysis of MLE. Assume we have  $K$  candidate models  $M_1, M_2, \dots, M_K$ , and each model  $M_k$  is characterized by a parametric probabilistic model  $P_k(y|\mathbf{x}; \boldsymbol{\theta}_k)$ , a prior distribution  $\pi_k(\boldsymbol{\theta}_k)$ , where  $\boldsymbol{\theta}_k \in \mathcal{W}_k \subset \mathbb{R}^{p_k}$  is the parameter vector. We demonstrate that AIC selects the model with the smallest population risk, and BIC identifies the true data-generating model by maximizing the marginal likelihood.

**AIC** This criterion [29] ranks statistical models based on the Kullback-Leibler (KL) divergence between the true data distribution  $P_Z$  and the learned parametric model. With  $\hat{\boldsymbol{\theta}}_{\text{ML}}^{(k)}$  denoting the MLE of the  $k$ th model, AIC selects the model as the solution to

$$\operatorname{argmin}_k D(P_Z \| P_k(y|\mathbf{x}; \hat{\boldsymbol{\theta}}_{\text{ML}}^{(k)})) = \operatorname{argmin}_k \mathbb{E}_{P_Z} [-\log P_k(y|\mathbf{x}; \hat{\boldsymbol{\theta}}_{\text{ML}}^{(k)})]. \quad (3)$$

The term  $\mathbb{E}_{P_Z} [-\log P_k(y|\mathbf{x}; \hat{\boldsymbol{\theta}}_{\text{ML}}^{(k)})]$  can be interpreted as the population risk  $L_P(\hat{\boldsymbol{\theta}}_{\text{ML}}^{(k)}, P_Z)$  of the MLE under log-loss. From this perspective, AIC measures how well the model fits the unknown data distribution  $P_Z$ , with smaller AIC values suggesting a lower population risk.

As the true distribution  $P_Z$  is unknown, the AIC is obtained by approximating the population risk as the sum of empirical risk, i.e., the negative log-likelihood of  $\hat{\boldsymbol{\theta}}_{\text{ML}}^{(k)}$  on training samples and a penalty term corresponding to the generalization error. In the classic regime where  $p_k$  is fixed and  $n \rightarrow \infty$ , the asymptotic normality of MLE yields

$$\text{AIC}(M_k) \triangleq -\frac{\hat{L}_k(\hat{\boldsymbol{\theta}}_{\text{ML}}^{(k)})}{n} + \frac{p_k}{n}, \quad \text{whence } \text{AIC} = -\frac{\hat{L}(\hat{\boldsymbol{\theta}}_{\text{ML}})}{n} + \frac{p}{n}. \quad (4)$$

Note that our form of AIC differs by a factor of 2 from its classical form to facilitate a direct comparison to population risk and generalization error as defined earlier in 2. Detailed derivations are provided, for reference, in Appendix A.

**BIC** This criterion [30] ranks statistical models by their marginal likelihoods of generating the data, with smaller values of the BIC correspond to larger marginal likelihoods. Approximating the marginal likelihood of observing  $\mathbf{z}^n$  for  $M_k$ , i.e.,  $m_k(\mathbf{z}^n) \triangleq \int P_k(y^n|\mathbf{x}^n; \boldsymbol{\theta}_k) \pi_k(\boldsymbol{\theta}_k) d\boldsymbol{\theta}_k$ , using Laplace's method yields

$$\log m_k(\mathbf{z}^n) = \hat{L}_k(\hat{\boldsymbol{\theta}}_{\text{ML}}^{(k)}) - \frac{p_k}{2} \log n + O(1), \quad n \rightarrow \infty. \quad (5)$$

In turn, BIC is obtained from (5) by dropping terms that don't scale with  $n$  and scaling by  $-1/n$ :

$$\text{BIC}(M_k) \triangleq -\frac{\hat{L}_k(\hat{\boldsymbol{\theta}}_{\text{ML}}^{(k)})}{n} + \frac{p_k \log n}{2n}, \quad \text{whence } \text{BIC} = -\frac{\hat{L}(\hat{\boldsymbol{\theta}}_{\text{ML}})}{n} + \frac{p \log n}{2n}. \quad (6)$$

When, further,  $P(M_k) = 1/K$ , we obtain

$$P(M_k | \mathbf{z}^n) = \frac{m_k(\mathbf{z}^n)P(M_k)}{\sum_{k=1}^K m_k(\mathbf{z}^n)P(M_k)} \propto m_k(\mathbf{z}^n). \quad (7)$$

Thus, when we assume a uniform prior over different models, the BIC ranks models by their posterior probability of generating the training data, and choosing the smallest BIC corresponds to the maximum a posteriori rule for model selection. A detailed derivation is provided in Appendix B.

Both (4) and (6) share a common first term, representing the average negative log-likelihood of the training data for MLE, which can be interpreted as the empirical risk with log-loss, decreasing as we adopt more complex models. We note that AIC and BIC in the classical  $n \rightarrow \infty$  regime are independent of the form of the model family  $P(y|\mathbf{x}; \boldsymbol{\theta})$  and the prior distribution  $\pi(\boldsymbol{\theta})$ , which makes it compatible with general distribution families subject to mild smoothness constraints. But because AIC and BIC differ in the second penalty term, they select different models.

## 2.2 Information Risk Minimization and Gibbs Algorithm

Classical AIC and BIC depend on MLE, which can be viewed as an ERM solution that only minimizes empirical risk. Instead, we motivate the Gibbs algorithm using an information risk minimization framework, which minimizes both empirical risk and a bound of generalization error.

We start with the following mutual information-based generalization error bound proposed in [31].

**Lemma 1** ([31]). *Suppose the loss function  $\ell(w, z) \in [0, 1]$  is bounded, and  $S = \{Z_i\}_{i=1}^n$  contains  $n$  i.i.d. training samples, then  $|\overline{gen}(P_{\hat{W}|S}, P_S)| \leq \sqrt{I(\hat{W}; S)/(2n)}$ .*

From Lemma 1, we know that the mutual information between training data  $S$  and the learned parameter  $\hat{W}$  can be used as an upper bound for generalization error. Thus, [31] further considers the following algorithm that minimizes empirical risks regularized with mutual information,

$$P_{\hat{W}|S}^* = \underset{P_{\hat{W}|S}}{\text{argmin}} \mathbb{E}_{P_{\hat{W},S}} [L_E(\hat{W}, S)] + \frac{1}{\beta} I(\hat{W}; S), \quad (8)$$

where  $\beta > 0$  controls the regularization term and balances between over-fitting and generalization. As  $\beta \rightarrow \infty$ , it reduces back to the standard ERM algorithm.

As computing  $I(\hat{W}; S)$  requires the knowledge of  $P_{\hat{W}}$ , [4, 31, 32] relax (8) by replacing it with an upper bound  $D(P_{\hat{W}|S} \| \pi | P_S) \geq I(\hat{W}; S)$ , where  $\pi$  is an arbitrary prior distribution over  $\mathcal{W}$ . The following lemma characterizes the solution to the relaxed problem.

**Lemma 2** ([4, 32]). *The minimum value of the following information risk minimization problem is*

$$\min_{P_{\hat{W}|S}} \mathbb{E}_{P_{\hat{W},S}} [L_E(\hat{W}, S)] + \frac{1}{\beta} D(P_{\hat{W}|S} \| \pi | P_S) = -\frac{1}{\beta} \mathbb{E}_{P_S} [\log \mathbb{E}_{\pi} [e^{-\beta L_E(W,S)}]], \quad (9)$$

which is achieved by the following Gibbs algorithm (distribution)

$$P_{\hat{W}|S}^*(w|s) = \frac{\pi(w)e^{-\beta L_E(w,s)}}{\mathbb{E}_{\pi} [e^{-\beta L_E(W,s)}]}, \quad \text{for } \beta > 0. \quad (10)$$

## 2.3 Gibbs Algorithm and SGLD

The Gibbs distribution was first proposed by [33] in statistical mechanics and further investigated by [34] in information theory. In general, it is difficult to compute directly due to the integral in the partition function  $\mathbb{E}_{\pi} [e^{-\beta L_E(W,s)}]$ . To address this issue, we use SGLD to obtain samples from the Gibbs distribution.

The SGLD algorithm is defined using the following update formula,

$$\hat{W}_{t+1} = \hat{W}_t - \eta \nabla L_E(\hat{W}_t, s) + \sqrt{\frac{2\eta}{\beta}} \zeta_t, \quad t = 0, 1, \dots, \quad (11)$$

where  $\zeta_t$  is a standard Gaussian random vector and  $\eta \geq 0$  is the step size. Thus, SGLD can also be viewed as a noisy version of standard SGD. It is shown in [35] that under some conditions on loss function, the Wasserstein distance between the distribution  $P_{\hat{W}_t|S}$  induced by SGLD and the Gibbs  $P_{\hat{W}|S} \propto \exp(-\beta L_E(\hat{W}, s))$  will converge to zero as  $t$  goes infinity. This allows us to sample the  $\hat{W}$  from the Gibbs distribution using SGLD with sufficiently large training steps  $t$ . Note that SGLD has been applied similarly to optimize generalization bound in [36]. A more detailed discussion of our implementation of SGLD can be found in Appendix C.

### 3 SGLD-based Information Criteria

We now develop information-theoretic analyses for SGLD-based AIC and BIC, following the same classical principles. AIC captures the population risk, and BIC approximates the log marginal likelihood. We demonstrate that our proposed SGLD-based information criteria align with the classical information criteria in the traditional large  $n$  regime and discuss how our information-theoretic analysis can be generalized to the over-parameterized regime.

#### 3.1 SGLD-based AIC

As we discussed in Section 2.1, the penalty term in AIC can be viewed as the generalization error of MLE with log-loss. Thus, we start with the following result from [5], which provides an exact characterization for the generalization error of the Gibbs algorithm using information measure.

**Proposition 1** ([5]). *For the Gibbs algorithm defined in (10), the expected generalization error is*

$$\overline{gen}(P_{\hat{W}|S}^*, P_S) = I_{\text{SKL}}(P_{\hat{W}|S}^*, P_S) / \beta, \quad (12)$$

where  $I_{\text{SKL}}(P_{\hat{W}|S}^*, P_S)$  is the symmetrized KL information between  $\hat{W}$  and  $S$ , defined as follows

$$I_{\text{SKL}}(P_{Y|X}, P_X) \triangleq D(P_{X,Y} \| P_X \otimes P_Y) + D(P_X \otimes P_Y \| P_{X,Y}). \quad (13)$$

Notably, information risk minimization in (8) regularizes the mutual information  $I(\hat{W}; S)$  as a proxy of the generalization error, but the exact generalization error of the Gibbs algorithm is the symmetrized KL information, which is always larger than the mutual information.

As discussed in Section 2.3, we can obtain samples from the Gibbs distribution by running SGLD until convergence. Thus, the population risk of the Gibbs algorithm can be approximated using the output of SGLD by  $L_P(w, P_Z) \approx L_E(\hat{W}_{\text{SGLD}}, z^n) + \frac{1}{\beta} I_{\text{SKL}}(P_{\hat{W}|S}^*, P_S)$ , which motivates the following proposed *SGLD-based AIC*:

$$\text{AIC}^+ \triangleq L_E(\hat{W}_{\text{SGLD}}, z^n) + \frac{1}{\beta} I_{\text{SKL}}(P_{\hat{W}|S}^*, P_S). \quad (14)$$

Observe that the penalty term in SGLD-based AIC is an information measure that characterizes the generalization error of the Gibbs algorithm. By investigating the asymptotic behavior of  $I_{\text{SKL}}(P_{\hat{W}|S}^*, P_S)$ , we have the following theorem characterizes the SGLD-based AIC in the classical asymptotic regime.

**Theorem 1.** *(proved in Appendix D) Consider the log-loss function  $\ell(w, z) = -\log P(y|x; w)$ , and set  $\beta = n$ . Under proper regularization assumptions in Appendix D, the SGLD-based AIC has the following form in the regime where  $p$  is fixed and  $n \rightarrow \infty$ :*

$$\text{AIC}^+ = L_E(\hat{W}_{\text{SGLD}}, z^n) + \frac{p}{n}. \quad (15)$$

Evidently, our information-theoretic analysis has the same AIC penalty term for the  $\text{AIC}^+$  in the classical regime, which suggests that the generalization error of the Gibbs algorithm (SGLD) has the same order of  $p/n$  as that of the MLE (SGD) in this regime.

### 3.2 SGLD-based BIC

The SGLD-based BIC is constructed by computing the marginal likelihood  $m(\mathbf{z}^n)$  using the information risk minimization framework. As such, it differs from the standard approach in classical (MLE-based) BIC, as no Laplace approximation is needed.

We now show that the minimum value achieved by the Gibbs algorithm with log-loss in the information risk minimization is the negative log-marginal likelihood.

**Proposition 2.** (proved in Appendix E) For the Gibbs algorithm  $P_{\hat{W}|S}^*$  defined in (10), if we adopt the log-loss function  $\ell(w, \mathbf{z}) = -\log P(y|\mathbf{x}; w)$ , and set  $\beta = n$ , the marginal likelihood is

$$-\frac{1}{n} \log m(\mathbf{z}^n) = \mathbb{E}_{P_{\hat{W}|S=\mathbf{z}^n}^*} [L_E(\hat{W}, \mathbf{z}^n)] + \frac{1}{n} D(P_{\hat{W}|S=\mathbf{z}^n}^* \|\pi). \quad (16)$$

Motivated by Proposition 2, we propose the SGLD-based BIC to approximate the marginal likelihood:

$$\text{BIC}^+ \triangleq L_E(\hat{W}_{\text{SGLD}}, \mathbf{z}^n) + \frac{1}{n} D(P_{\hat{W}|S=\mathbf{z}^n}^* \|\pi). \quad (17)$$

To compare it with the classical BIC, it suffices to investigate the asymptotic behavior of the KL divergence between the Gibbs posterior distribution and the prior as  $n \rightarrow \infty$ . The final expression of the SGLD-based BIC is formally stated in the following Theorem.

**Theorem 2.** (proved in Appendix F) Under proper regularization assumptions in Appendix F, the SGLD-based BIC has the following form in the classical regime where  $p$  is fixed and  $n \rightarrow \infty$ ,

$$\text{BIC}^+ \triangleq L_E(\hat{W}_{\text{SGLD}}, \mathbf{z}^n) + \frac{p}{2n} \log n. \quad (18)$$

As expected, we have the same BIC penalty term for the  $\text{BIC}^+$  in the classical regime. The experimental results in Section 5.1 show that the proposed SGLD-based AIC and BIC are comparable to their classic counterparts. In the over-parameterized regimes, they are not, as we now develop.

## 4 BIC for Over-Parameterized RF Model

As shown in Figure 1 (right), the classical AIC and BIC fail to capture the double-descent trend exhibited by the test MSE of the RF model. This is due to the fact that the generalization error and marginal likelihood have different behaviors in the over-parameterized regime, which cannot be characterized by the classical asymptotic analysis. The classical analyses heavily rely on the asymptotic normality of MLE and Laplace approximation under certain regularization assumptions, which ignores the prior distribution as  $n \rightarrow \infty$ . Unfortunately, none of these properties hold in the over-parameterized regime where  $p \gg n$ , as there exist an infinite number of possible model parameters that could interpolate  $n$  samples perfectly, making the classical AIC and BIC ill-defined.

However, the SGLD-based  $\text{AIC}^+$  in (14) and  $\text{BIC}^+$  in (17) defined using different information measures can be generalized to over-parameterized models, as Proposition 1 and 2 hold regardless of the values of  $p$  and  $n$ . Since  $\text{AIC}^+$  mainly captures the generalization error of the Gibbs algorithm, which can be estimated using validation data in practice, our focus lies in extending the analysis of  $\text{BIC}^+$  to approximate the marginal likelihood in the over-parameterized regime.

Owing to the complex nature of fitting in the over-parameterized regime, we do not pursue a general asymptotic formula that applies to various model architectures, as in the classic regime. Instead, we refine the SGLD-based  $\text{BIC}^+$  analysis to this regime for the random feature (RF) model.

### 4.1 Random Feature Model

The RF model [37] takes the form of two-layer neural network with fixed random weights in the first layer. Specifically, the output of RF model with input data  $\mathbf{x} \in \mathbb{R}^d$  is

$$g(\mathbf{x}) \triangleq \sum_{j=1}^p f\left(\frac{\langle \mathbf{x}, \mathbf{F}_j \rangle}{\sqrt{d}}\right) \mathbf{w}_j = f\left(\frac{\mathbf{x}^\top \mathbf{F}}{\sqrt{d}}\right) \mathbf{w}, \quad (19)$$

where  $\mathbf{w} \in \mathbb{R}^p$  denotes the weights of the model. Moreover,  $\mathbf{F}_j \in \mathbb{R}^d$  denotes the  $j$ th random feature vector, which is the  $j$ th column of the random feature matrix  $\mathbf{F} \in \mathbb{R}^{d \times p}$  whose entries are drawn i.i.d. from  $\mathcal{N}(0, 1)$ . Finally,  $f(\cdot)$  is a point-wise activation function. In our setting, there are  $n$  training samples  $\mathbf{z}^n = \{(\mathbf{x}_i, y_i)\}_{i=1}^n$ , and the  $\mathbf{x}_i$  are drawn i.i.d. from  $\mathcal{N}(0, \mathbf{I}_d)$ .

The parametric distribution family induced by the random feature model takes the form

$$P(y^n | \mathbf{x}^n; \mathbf{w}) = \frac{1}{(2\pi\sigma^2)^{n/2}} \exp\left(-\frac{1}{2\sigma^2} \sum_{i=1}^n (y_i - f(\frac{\mathbf{x}_i^\top \mathbf{F}}{\sqrt{d}}) \mathbf{w})^2\right), \quad (20)$$

with a fixed random feature matrix  $\mathbf{F}$ , and a Gaussian prior distribution  $\mathbf{w} \sim \mathcal{N}(0, \frac{\sigma^2}{\lambda n} \mathbf{I}_p)$ . The weights of the RF model  $\mathbf{w}$  can be trained by performing SGLD on the regularized log-loss

$$\mathcal{L}(\mathbf{w}) = \frac{1}{2\sigma^2} \|\mathbf{Y} - \mathbf{B}\mathbf{w}\|_2^2 + \frac{n}{2} \log(2\pi\sigma^2) + \frac{\lambda n \|\mathbf{w}\|_2^2}{2\sigma^2}, \quad \text{where } \mathbf{B} \triangleq f(\mathbf{X}\mathbf{F}/\sqrt{d}) \in \mathbb{R}^{n \times p}, \quad (21)$$

and we collect the training data in a matrix  $\mathbf{X} \in \mathbb{R}^{n \times d}$  and a vector  $\mathbf{Y} \in \mathbb{R}^n$  to simplify the notation.

As discussed in [18, 25], a significant benefit of using the random feature model is that, unlike in standard linear regression, the dimensionality of the input data  $d$  is not entangled with the number of parameters  $p$ .

## 4.2 SGLD-based BIC for Over-Parameterized RF Model

To generalize BIC<sup>+</sup> to the over-parameterized RF model, it suffices to focus on the second KL-divergence term in 17. In the random feature model, it can be shown (see Appendix G for details) that the Gibbs algorithm reduces to the Gaussian posterior distribution  $P_{\hat{W}|S}^* \sim \mathcal{N}(\hat{W}_\lambda, \Sigma_w)$ , with  $\hat{W}_\lambda = (\lambda n \mathbf{I}_p + \mathbf{B}^\top \mathbf{B})^{-1} \mathbf{B}^\top \mathbf{Y}$ , and  $\Sigma_w = \sigma^2 (\lambda n \mathbf{I}_p + \mathbf{B}^\top \mathbf{B})^{-1}$ .

Thus, the KL-divergence between the Gibbs posterior distribution and prior  $\mathcal{N}(0, \frac{\sigma^2}{\lambda n} \mathbf{I}_p)$  is given by

$$D(P_{\hat{W}|S=z^n}^* \|\pi) = \frac{1}{2} \left[ \frac{\lambda n}{\sigma^2} \|\hat{W}_\lambda\|_2^2 + \log \frac{\det(\frac{\sigma^2}{\lambda n} \mathbf{I}_p)}{\det(\Sigma_w)} + \text{tr}(\frac{\lambda n}{\sigma^2} \Sigma_w) - p \right]. \quad (22)$$

Note that the  $\ell_2$  norm of  $\hat{W}_\lambda$  can be approximated using  $\hat{W}_{\text{SGLD}}$  in practice. To obtain a convenient expression for the remaining determinant and trace terms, we first impose restrictions on the activation function  $f(\cdot)$ . Therefore, these two terms can be characterized using random matrix theory by studying the eigenvalues of  $\Sigma \triangleq \mathbf{B}^\top \mathbf{B} / (\lambda n) + \mathbf{I}_p$  in the over-parameterized regime. In particular, for activation functions  $f(\cdot)$  that satisfy conditions

$$\mathbb{E}[f(\varepsilon)] = 0, \quad \mathbb{E}[f(\varepsilon)^2] = 1, \quad \mathbb{E}[f'(\varepsilon)] = 0, \quad |\mathbb{E}[f(\varepsilon)^k]| < \infty, \quad \text{for } k > 1, \quad (23)$$

where  $\varepsilon \sim \mathcal{N}(0, 1)$ , the following theorem characterizes the KL divergence term in the over-parameterized RF model.

**Theorem 3.** *For activation functions  $f(\cdot)$  satisfying the conditions in (23), as  $n, d, p \rightarrow \infty$  with  $p/d \rightarrow r_1$ ,  $n/d \rightarrow r_2$ , and  $r_1/r_2 = r$ , where  $r_1, r_2 \in (0, \infty)$ , we have*

$$\frac{1}{n} D(P_{\hat{W}|S=z^n}^* \|\pi) \rightarrow \frac{\lambda}{2\sigma^2} \|\hat{W}_\lambda\|_2^2 - \frac{\lambda}{8} \mathcal{F}(\frac{1}{\lambda}, r) + \frac{1}{2} V(1/\lambda, r) \quad (24)$$

almost surely, where

$$V(\gamma, r) \triangleq r \log \left(1 + \gamma - \frac{1}{4} \mathcal{F}(\gamma, r)\right) - \frac{1}{4\gamma} \mathcal{F}(\gamma, r) + \log \left(1 + \gamma r - \frac{1}{4} \mathcal{F}(\gamma, r)\right), \quad (25)$$

with

$$\mathcal{F}(\gamma, r) \triangleq \left( \sqrt{\gamma(1 + \sqrt{r})^2 + 1} - \sqrt{\gamma(1 - \sqrt{r})^2 + 1} \right)^2. \quad (26)$$

*Sketch of Proof.* The proof is based on the results from [38], which shows that the distribution of the eigenvalues of the random matrix  $\mathbf{B}^\top \mathbf{B} / n$  converges to the Marchenko-Pastur distribution with shape parameter  $r$  (a well-studied distribution in random matrix theory [39]). The detailed proof is provided in Appendix H.  $\square$

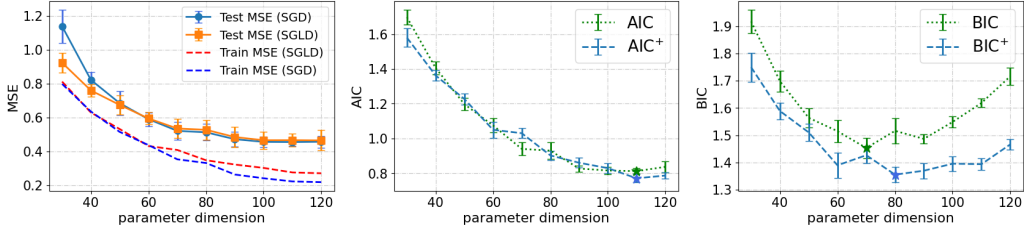


Figure 2: A comparison of SGD and SGLD in terms of MSE (**left**). Comparisons of the classical AIC with AIC<sup>+</sup> in (15) (**middle**), and the classical BIC with BIC<sup>+</sup> in (18) (**right**). All experiments are conducted in the classical  $n \gg p$  setting, with  $n = 600$ ,  $p = [30, \dots, 120]$ . The preferred models selected by different information criteria are marked using stars with different colors.

**Remark 1.** An example of an activation function that satisfies all the assumptions we made in (23) is  $f(x) = (x^2 - 1)/\sqrt{2}$ . More examples of such activation functions can be found in [38]. We further note that the assumption  $\mathbb{E}[f'(\varepsilon)] = 0$  on the activation function is used only to obtain a simple closed-form for the KL divergence, a more general result by considering the Stieltjes transform of  $\mathbf{B}^\top \mathbf{B}/n$  for other activation functions is provided in Appendix H.

Theorem 3 motivates us to define the following SGLD-based BIC for the over-parameterized RF model to approximate the marginal likelihood,

$$\text{BIC}^+ \triangleq L_E(\hat{W}_{\text{SGLD}}, z^n) + \frac{\lambda}{2\sigma^2} \|\hat{W}_{\text{SGLD}}\|_2^2 - \frac{\lambda}{8} \mathcal{F}\left(\frac{1}{\lambda}, r\right) + \frac{1}{2} V(1/\lambda, r). \quad (27)$$

The penalty term consists of the  $\ell_2$  norm of the learned weights, and two other terms capture the log determinant and trace in the over-parameterized regime, which will be referred to as the covariance term altogether in the next section.

## 5 Experiments

In this section, we first evaluate both the SGLD-based AIC and BIC for the RF model in the classical regime, and the proposed BIC<sup>+</sup> in the over-parameterized RF model. See Appendix I for details and additional experimental results.

### 5.1 Classic Regime

We instantiate a two-layer RF model described in (19), where the first layer is designated for feature mapping and is kept random, and we only train the parameter in the second layer. We use the regularized negative log-likelihood in (21) as the loss function for SGLD to compute both AIC<sup>+</sup> in (15) and BIC<sup>+</sup> in (18), which is different from the SGD algorithm used in classical AIC and BIC.

For simplicity, we generate  $n = 600$  training samples from this linear model

$$y_i = \mathbf{x}_i^\top \mathbf{w}^* + \varepsilon_i, \quad \mathbf{w}^* \in \mathbb{R}^p, \quad \|\mathbf{w}^*\|_2^2 = 1, \quad \varepsilon_i \sim \mathcal{N}(0, \sigma^2), \quad (28)$$

with  $p = 80$ , and noise  $\sigma^2 = 0.2$ .

In Figure 2 (Left), we plot the training and test MSEs achieved using SGD and SGLD, respectively. Although SGD and SGLD might yield different model parameters, they exhibit a similar trend in terms of MSE and Log-Loss (see Appendix I). The discrepancy in the training algorithms does not significantly impact model selection. Figure 2 (middle) demonstrates that both AIC and AIC<sup>+</sup> follow a similar trend to the test MSE, selecting the model ( $p = 110$ ) that achieves the smallest population risk. On the other hand, due to larger penalty terms, BIC and BIC<sup>+</sup> favor simpler models and identify the model most likely to generate the training data. As shown in Figure 2 (right), the classical BIC selects the model with  $p = 70$ , while BIC<sup>+</sup> favors the model with  $p = 80$ . In summary, our observations suggest that AIC<sup>+</sup> and BIC<sup>+</sup> based on SGLD exhibit similar model selection capabilities to the traditional AIC and BIC in the classical large  $n$  regime.

### 5.2 Over-parameterized Regime

In the over-parameterized regime, we evaluate the SGLD based BIC<sup>+</sup> using  $n = 200$  samples generated by the same linear model in (28), with  $p = 400$  and noise  $\sigma^2 = 1.2$ . To make the double

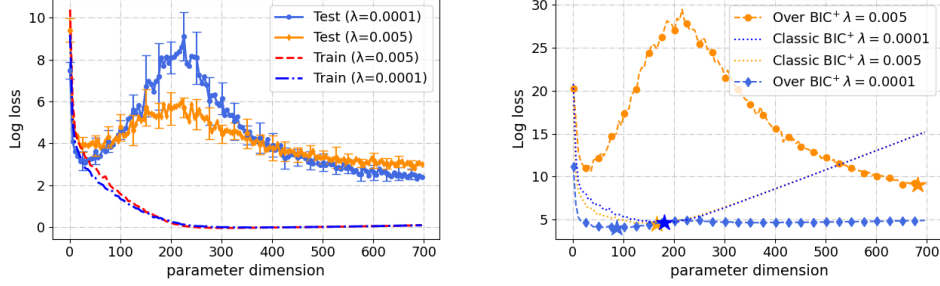


Figure 3: A comparison of the log loss achieved by SGLD with varying regularizer  $\lambda$  (**left**). A comparison of  $\text{BIC}^+$  in the over-parameterized and classical regime with varying  $\lambda$  (**right**). The preferred models selected by different information criteria are marked using stars.

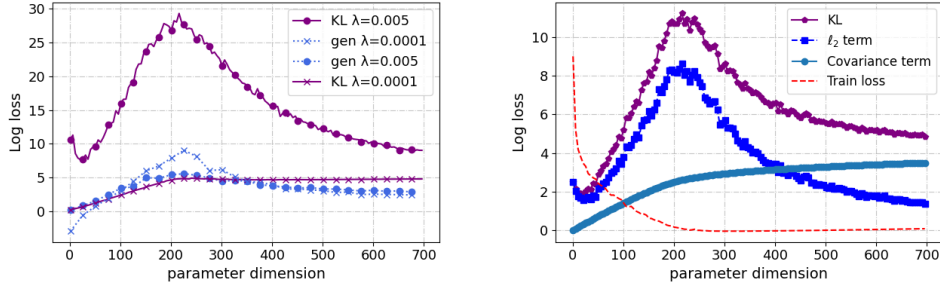


Figure 4: A comparison between the KL-divergence term in  $\text{BIC}^+$  and the generalization error term in  $\text{AIC}^+$  with varying  $\lambda$  (**left**). A decomposition of the four terms in over-parameterized  $\text{BIC}^+$  in (27) with  $\lambda = 0.001$  (**right**).

descent phenomenon more evident, we increase the variance of the noise as suggested in [10]. We conduct experiments with different regularizers  $\lambda$  to understand the influence of prior distributions.

As depicted in Figure 1 (left) and Figure 3 (left), the peaks of test MSE and Log-Loss are located at the interpolation threshold, i.e., when  $p = n = 200$ , resulting in the highest generalization error. As  $p$  continues to increase, the test error begins to decline again, even falling below the levels observed in the under-parameterized regime  $p < n$ . In the right panel of Figure 3, it is evident that the  $\text{BIC}^+$  in (18) fails to capture the double descent, whereas the over-parameterized  $\text{BIC}^+$  in (27) succeeds.

Figure 3 (left) also demonstrates that when  $\lambda$  is larger, the double descent phenomenon is less obvious. However, the over-parameterized  $\text{BIC}^+$  behaves in an opposite way, as shown in Figure 3 (right). This is because that a larger  $\lambda$  induces a more concentrated prior distribution  $\mathcal{N}(0, \sigma^2/(\lambda n)\mathbf{I}_p)$ . The posterior distribution  $P_{\hat{W}|S=z^n}^*$ , which needs to fit the data, concentrates at a slower rate compared to the prior distribution. As a result, the KL divergence term in  $\text{BIC}^+$  increases as  $\lambda$  increases. Note that a similar mismatch between marginal likelihood and generalization has been observed in [28].

We further investigate this inconsistency between the KL divergence and the generalization error in Figure 4 (left). Unlike the classical BIC, where the penalty term  $(p/(2n))\log n$  is order-wise larger than the  $p/n$  term in classical AIC, it can be seen that the KL divergence term in the over-parameterized  $\text{BIC}^+$  can be smaller than the generalization error ( $I_{\text{SKL}}$  in  $\text{AIC}^+$ ), depending on the value of  $\lambda$  and  $p$ . Thus, the mismatch between marginal likelihood (BIC) and population risk (AIC) is even more complicated in the over-parameterized setting due to the influence of prior distribution.

In Figure 4 (right), we decompose the penalty term of the over-parameterized  $\text{BIC}^+$  in (27) into  $\ell_2$  term, covariance term, and the training loss. When  $p \leq n$ , the model prior can be ignored, and the training loss becomes the dominant factor of  $\text{BIC}^+$ . In this case, the KL divergence and the covariance term increase with  $p$ , corresponding to the classical BIC. When  $p \geq n$ , the double descent behavior of the  $\ell_2$  norm term dominates the over-parameterized  $\text{BIC}^+$ . In this regime, multiple weights exist that can fit the training data perfectly. We observe that the  $\ell_2$  norm of the SGLD solution decreases as  $p$  increases, which implies that SGLD prefers the weights with smaller  $\ell_2$  norm. Note that similar phenomena are observed for SGD, and generalization error bounds using different weights norms are established in [40, 41], which shows the profound connection of the double descent between generalization error (AIC) and the marginal likelihood (BIC).

## References

- [1] S. Geman, E. Bienenstock, and R. Doursat, “Neural networks and the bias/variance dilemma,” *Neural Computation*, vol. 4, no. 1, pp. 1–58, 1992.
- [2] C. Zhang, S. Bengio, M. Hardt, B. Recht, and O. Vinyals, “Understanding deep learning requires rethinking generalization,” in *Proc. International Conference on Learning Representations (ICLR)*, 2017.
- [3] M. Belkin, D. Hsu, S. Ma, and S. Mandal, “Reconciling modern machine-learning practice and the classical bias–variance trade-off,” *Proceedings of the National Academy of Sciences*, vol. 116, no. 32, pp. 15849–15854, 2019.
- [4] T. Zhang, “Information-theoretic upper and lower bounds for statistical estimation,” *IEEE Transactions on Information Theory*, vol. 52, no. 4, pp. 1307–1321, 2006.
- [5] G. Aminian, Y. Bu, L. Toni, M. Rodrigues, and G. Wornell, “An exact characterization of the generalization error for the Gibbs algorithm,” *Advances in Neural Information Processing Systems*, vol. 34, pp. 8106–8118, 2021.
- [6] J. Chen and Z. Chen, “Extended Bayesian information criteria for model selection with large model spaces,” *Biometrika*, vol. 95, no. 3, pp. 759–771, 2008.
- [7] Y. Fan and C. Y. Tang, “Tuning parameter selection in high dimensional penalized likelihood,” *Journal of the Royal Statistical Society: SERIES B: Statistical Methodology*, pp. 531–552, 2013.
- [8] M. S. Advani, A. M. Saxe, and H. Sompolinsky, “High-dimensional dynamics of generalization error in neural networks,” *Neural Networks*, 2020.
- [9] M. Geiger, S. Spigler, S. d’Ascoli, L. Sagun, M. Baity-Jesi, G. Biroli, and M. Wyart, “Jamming transition as a paradigm to understand the loss landscape of deep neural networks,” *Physical Review E*, vol. 100, no. 1, p. 012115, 2019.
- [10] P. Nakkiran, G. Kaplun, Y. Bansal, T. Yang, B. Barak, and I. Sutskever, “Deep double descent: Where bigger models and more data hurt,” in *International Conference on Learning Representations*, 2019.
- [11] M. Belkin, D. Hsu, and J. Xu, “Two models of double descent for weak features,” *SIAM Journal on Mathematics of Data Science*, vol. 2, pp. 1167–1180, jan 2020.
- [12] T. Hastie, A. Montanari, S. Rosset, and R. J. Tibshirani, “Surprises in high-dimensional ridgeless least squares interpolation,” *The Annals of Statistics*, vol. 50, no. 2, pp. 949–986, 2022.
- [13] P. L. Bartlett, P. M. Long, G. Lugosi, and A. Tsigler, “Benign overfitting in linear regression,” *Proceedings of the National Academy of Sciences*, 2020.
- [14] V. Muthukumar, K. Vodrahalli, V. Subramanian, and A. Sahai, “Harmless interpolation of noisy data in regression,” *IEEE Journal on Selected Areas in Information Theory*, 2020.
- [15] Z. Deng, A. Kammoun, and C. Thrampoulidis, “A model of double descent for high-dimensional binary linear classification,” *Information and Inference: A Journal of the IMA*, vol. 11, no. 2, pp. 435–495, 2022.
- [16] G. R. Kini and C. Thrampoulidis, “Analytic study of double descent in binary classification: The impact of loss,” in *2020 IEEE International Symposium on Information Theory (ISIT)*, pp. 2527–2532, IEEE, 2020.
- [17] F. Gerace, B. Loureiro, F. Krzakala, M. Mézard, and L. Zdeborová, “Generalisation error in learning with random features and the hidden manifold model,” in *International Conference on Machine Learning*, pp. 3452–3462, PMLR, 2020.
- [18] S. Mei and A. Montanari, “The generalization error of random features regression: Precise asymptotics and the double descent curve,” *Communications on Pure and Applied Mathematics*, vol. 75, no. 4, pp. 667–766, 2022.
- [19] S. d’Ascoli, M. Refinetti, G. Biroli, and F. Krzakala, “Double trouble in double descent: Bias and variance (s) in the lazy regime,” in *International Conference on Machine Learning*, pp. 2280–2290, PMLR, 2020.
- [20] E. Weinan, C. Ma, and L. Wu, “A comparative analysis of optimization and generalization properties of two-layer neural network and random feature models under gradient descent dynamics,” *Science China Mathematics*, pp. 1–24, 2020.

- [21] F. Liu, J. Suykens, and V. Cevher, “On the double descent of random features models trained with SGD,” *Advances in Neural Information Processing Systems*, vol. 35, pp. 34966–34980, 2022.
- [22] Z. Yang, Y. Yu, C. You, J. Steinhardt, and Y. Ma, “Rethinking bias-variance trade-off for generalization of neural networks,” in *International Conference on Machine Learning*, pp. 10767–10777, PMLR, 2020.
- [23] R. Dwivedi, C. Singh, B. Yu, and M. J. Wainwright, “Revisiting complexity and the bias-variance tradeoff,” *arXiv preprint arXiv:2006.10189*, 2020.
- [24] P. Nakkiran, “More data can hurt for linear regression: Sample-wise double descent,” *arXiv preprint arXiv:1912.07242*, 2019.
- [25] S. d’Ascoli, L. Sagun, and G. Biroli, “Triple descent and the two kinds of overfitting: Where & why do they appear?,” *Advances in Neural Information Processing Systems*, vol. 33, pp. 3058–3069, 2020.
- [26] R. Heckel and F. F. Yilmaz, “Early stopping in deep networks: Double descent and how to eliminate it,” *arXiv preprint arXiv:2007.10099*, 2020.
- [27] A. Immer, M. Bauer, V. Fortuin, G. Rätsch, and K. M. Emtiyaz, “Scalable marginal likelihood estimation for model selection in deep learning,” in *International Conference on Machine Learning*, pp. 4563–4573, PMLR, 2021.
- [28] S. Lotfi, P. Izmailov, G. Benton, M. Goldblum, and A. G. Wilson, “Bayesian model selection, the marginal likelihood, and generalization,” in *International Conference on Machine Learning*, pp. 14223–14247, PMLR, 2022.
- [29] H. Akaike, “Likelihood of a model and information criteria,” *Journal of Econometrics*, vol. 16, no. 1, pp. 3–14, 1981.
- [30] G. Schwarz *et al.*, “Estimating the dimension of a model,” *The annals of statistics*, vol. 6, no. 2, pp. 461–464, 1978.
- [31] A. Xu and M. Raginsky, “Information-theoretic analysis of generalization capability of learning algorithms,” in *Proc. Advances in Neural Information Processing Systems (NIPS)*, pp. 2524–2533, 2017.
- [32] S. M. Perlaza, G. Bisson, I. Esnaola, A. Jean-Marie, and S. Rini, “Empirical risk minimization with relative entropy regularization: Optimality and sensitivity analysis,” in *2022 IEEE International Symposium on Information Theory (ISIT)*, pp. 684–689, IEEE, 2022.
- [33] J. W. Gibbs, “Elementary principles of statistical mechanics,” *Compare*, vol. 289, p. 314, 1902.
- [34] E. T. Jaynes, “Information theory and statistical mechanics,” *Physical review*, vol. 106, no. 4, p. 620, 1957.
- [35] M. Raginsky, A. Rakhlin, and M. Telgarsky, “Non-convex learning via stochastic gradient Langevin dynamics: a nonasymptotic analysis,” in *Conference on Learning Theory*, pp. 1674–1703, PMLR, 2017.
- [36] G. K. Dziugaite and D. Roy, “Entropy-SGD optimizes the prior of a PAC-Bayes bound: Generalization properties of Entropy-SGD and data-dependent priors,” in *International Conference on Machine Learning*, pp. 1377–1386, PMLR, 2018.
- [37] A. Rahimi and B. Recht, “Random features for large-scale kernel machines,” in *Advances in neural information processing systems*, pp. 1177–1184, 2008.
- [38] J. Pennington and P. Worah, “Nonlinear random matrix theory for deep learning,” in *Advances in Neural Information Processing Systems*, pp. 2637–2646, 2017.
- [39] A. M. Tulino, S. Verdú, and S. Verdú, *Random matrix theory and wireless communications*. Now Publishers Inc, 2004.
- [40] B. Neyshabur, S. Bhojanapalli, D. McAllester, and N. Srebro, “Exploring generalization in deep learning,” *Advances in neural information processing systems*, vol. 30, 2017.
- [41] P. L. Bartlett, D. J. Foster, and M. J. Telgarsky, “Spectrally-normalized margin bounds for neural networks,” *Advances in neural information processing systems*, vol. 30, 2017.
- [42] A. W. Van der Vaart, *Asymptotic statistics*, vol. 3. Cambridge university press, 2000.

- [43] B. J. Kleijn, A. W. van der Vaart, *et al.*, “The Bernstein-von-Mises theorem under misspecification,” *Electronic Journal of Statistics*, vol. 6, pp. 354–381, 2012.
- [44] D. P. Palomar and S. Verdú, “Lautum information,” *IEEE transactions on information theory*, vol. 54, no. 3, pp. 964–975, 2008.
- [45] K. P. Murphy, “Conjugate bayesian analysis of the gaussian distribution,” *def*, vol. 1, no.  $2\sigma^2$ , p. 16, 2007.

## A Derivation of classical AIC

We start by formally presenting the regularization conditions required for the standard asymptotic normality of MLE in the classical regime.

### Assumption 1. Regularity Conditions for MLE

1. *Identifiability:*  $P(y|\mathbf{x};\boldsymbol{\theta}) \neq P(y|\mathbf{x};\boldsymbol{\theta}')$  for  $\boldsymbol{\theta} \neq \boldsymbol{\theta}'$ .
2.  $\Theta$  is an open subset of  $\mathbb{R}^p$ .
3. The function  $\log P(y|\mathbf{x};\boldsymbol{\theta})$  is three times continuously differentiable with respect to  $\boldsymbol{\theta}$ .
4. There exist functions  $F_1(z) : \mathcal{Z} \rightarrow \mathbb{R}, F_2(z) : \mathcal{Z} \rightarrow \mathbb{R}$  and  $M(z) : \mathcal{Z} \rightarrow \mathbb{R}$ , such that

$$\mathbb{E}_{Z \sim P(\mathbf{z};\boldsymbol{\theta})} [M(Z)] < \infty,$$

and the following inequalities hold for any  $\boldsymbol{\theta} \in \Theta$ ,

$$\begin{aligned} \left| \frac{\partial \log P(y|\mathbf{x};\boldsymbol{\theta})}{\partial \theta_i} \right| &< F_1(z), & \left| \frac{\partial^2 \log P(y|\mathbf{x};\boldsymbol{\theta})}{\partial \theta_i \partial \theta_j} \right| &< F_1(z), \\ \left| \frac{\partial^3 \log P(y|\mathbf{x};\boldsymbol{\theta})}{\partial \theta_i \partial \theta_j \partial \theta_k} \right| &< M(z), & i, j, k = 1, 2, \dots, p. \end{aligned}$$

5. The following inequality holds for an arbitrary  $\boldsymbol{\theta} \in \Theta$  and  $i, j = 1, 2, \dots, p$ ,

$$0 < \mathbb{E} \left[ \frac{\partial \log P(y|\mathbf{x};\boldsymbol{\theta})}{\partial \theta_i} \frac{\partial \log P(y|\mathbf{x};\boldsymbol{\theta})}{\partial \theta_j} \right] < \infty.$$

In the following, we provide proof of the classical AIC for reference.

The AIC model selection in (3) is equivalent to:

$$\operatorname{argmin}_k \mathbb{E}_{P_Z} [-\log P_k(y|\mathbf{x};\hat{\boldsymbol{\theta}}_{\text{ML}}^{(k)})] = \operatorname{argmin}_k \mathbb{E}_{P_S} [L_E(\hat{\boldsymbol{\theta}}_{\text{ML}}^{(k)}, S)] + \overline{gen}(\hat{\boldsymbol{\theta}}_{\text{ML}}^{(k)}, P_Z). \quad (29)$$

As  $n \rightarrow \infty$ , under the above regularization conditions, which guarantee that  $\hat{\boldsymbol{\theta}}_{\text{ML}}$  is unique, the asymptotic normality of the MLE states that the distribution of  $\hat{\boldsymbol{\theta}}_{\text{ML}}$  converges to

$$\mathcal{N}(\boldsymbol{\theta}^*, \frac{1}{n} J(\boldsymbol{\theta}^*)^{-1} I(\boldsymbol{\theta}^*) J(\boldsymbol{\theta}^*)^{-1}), \text{ with } \boldsymbol{\theta}^* \triangleq \operatorname{argmin}_{\boldsymbol{\theta} \in \Theta} D(P_Z \| P(y|\mathbf{x};\boldsymbol{\theta})), \quad (30)$$

where

$$J(\boldsymbol{\theta}) \triangleq \mathbb{E}_{P_Z} [-\nabla_{\boldsymbol{\theta}}^2 \log P(y|\mathbf{x};\boldsymbol{\theta})] \text{ and } I(\boldsymbol{\theta}) \triangleq \mathbb{E}_{P_Z} [\nabla_{\boldsymbol{\theta}} \log P(y|\mathbf{x};\boldsymbol{\theta}) \nabla_{\boldsymbol{\theta}} \log P(y|\mathbf{x};\boldsymbol{\theta})^\top]. \quad (31)$$

When the true model is in the parametric family  $P_Z = P(y|\mathbf{x};\boldsymbol{\theta}^*)$ , we have  $J(\boldsymbol{\theta}^*) = I(\boldsymbol{\theta}^*)$ , which is the Fisher information matrix.

Thus, the generalization term can be written as

$$\begin{aligned} -\overline{gen}(\hat{\boldsymbol{\theta}}_{\text{ML}}, P_Z) &= \mathbb{E}_{P_S} [L_E(\hat{\boldsymbol{\theta}}_{\text{ML}}, S)] - L_P(\hat{\boldsymbol{\theta}}_{\text{ML}}, P_Z) \\ &= \mathbb{E}_{P_S} [L_E(\hat{\boldsymbol{\theta}}_{\text{ML}}, S)] - \mathbb{E}_{P_S} [L_E(\boldsymbol{\theta}^*, S)] + \mathbb{E}_{P_S} [L_E(\boldsymbol{\theta}^*, S)] - L_P(\hat{\boldsymbol{\theta}}_{\text{ML}}, P_Z) \\ &= \mathbb{E}_{P_S} [L_E(\hat{\boldsymbol{\theta}}_{\text{ML}}, S) - L_E(\boldsymbol{\theta}^*, S)] + L_P(\boldsymbol{\theta}^*, P_Z) - L_P(\hat{\boldsymbol{\theta}}_{\text{ML}}, P_Z). \end{aligned} \quad (32)$$

As  $\hat{\boldsymbol{\theta}}_{\text{ML}}$  minimizes  $L_E(\hat{\boldsymbol{\theta}}_{\text{ML}}, S)$ , we take the Taylor expansion of  $L_E(\boldsymbol{\theta}^*, S)$  around the point  $\hat{\boldsymbol{\theta}}_{\text{ML}}$

$$L_E(\boldsymbol{\theta}^*, S) = L_E(\hat{\boldsymbol{\theta}}_{\text{ML}}, S) + \frac{1}{2}(\boldsymbol{\theta}^* - \hat{\boldsymbol{\theta}}_{\text{ML}})^\top J(\hat{\boldsymbol{\theta}}_{\text{ML}})(\boldsymbol{\theta}^* - \hat{\boldsymbol{\theta}}_{\text{ML}}) + \dots \quad (33)$$

And the Taylor expansion of  $L_P(\hat{\boldsymbol{\theta}}_{\text{ML}}, P_Z)$  around  $\boldsymbol{\theta}^*$  yields

$$L_P(\hat{\boldsymbol{\theta}}_{\text{ML}}, P_Z) = L_P(\boldsymbol{\theta}^*, P_Z) + \frac{1}{2}(\boldsymbol{\theta}^* - \hat{\boldsymbol{\theta}}_{\text{ML}})^\top J(\boldsymbol{\theta}^*)(\boldsymbol{\theta}^* - \hat{\boldsymbol{\theta}}_{\text{ML}}) + \dots \quad (34)$$

If we use the quadratic approximation of (33) and (34) in (32), we can get the following asymptotic expression for the generalization error

$$\overline{gen}(\hat{\boldsymbol{\theta}}_{\text{ML}}, P_Z) = \frac{1}{n} \text{tr}(I(\boldsymbol{\theta}^*)J(\boldsymbol{\theta}^*)^{-1}), \quad (35)$$

where the last step is due to the asymptotic normality of the MLE, and  $J(\hat{\boldsymbol{\theta}}_{\text{ML}})$  will converge to its expectation by the consistency of MLE and the strong law of large numbers. For the case where the true model is in the parametric family  $P_Z = P(y|\mathbf{x}; \boldsymbol{\theta}^*)$ ,  $J(\boldsymbol{\theta}^*) = I(\boldsymbol{\theta}^*)$ ,  $\overline{gen}(\hat{\boldsymbol{\theta}}_{\text{ML}}, P_Z) = p/n$ . Thus, plug the asymptotic generalization error term back in (29) can get,

$$\text{AIC} = -\frac{\hat{L}(\hat{\boldsymbol{\theta}}_{\text{ML}})}{n} + \frac{p}{n}. \quad (36)$$

## B Derivation of classical BIC

The Taylor expansion of the log-likelihood function  $\hat{L}(\boldsymbol{\theta})$  around  $\hat{\boldsymbol{\theta}}_{\text{ML}}$  yields

$$\hat{L}(\boldsymbol{\theta}) = \hat{L}(\hat{\boldsymbol{\theta}}_{\text{ML}}) - \frac{n}{2}(\boldsymbol{\theta} - \hat{\boldsymbol{\theta}}_{\text{ML}})^\top J(\hat{\boldsymbol{\theta}}_{\text{ML}})(\boldsymbol{\theta} - \hat{\boldsymbol{\theta}}_{\text{ML}}) + \dots \quad (37)$$

Similarly, we can expand the prior distribution  $\pi(\boldsymbol{\theta})$  with Taylor series around  $\hat{\boldsymbol{\theta}}_{\text{ML}}$  as

$$\pi(\boldsymbol{\theta}) = \pi(\hat{\boldsymbol{\theta}}_{\text{ML}}) + (\boldsymbol{\theta} - \hat{\boldsymbol{\theta}}_{\text{ML}})^\top \nabla \pi(\boldsymbol{\theta})|_{\boldsymbol{\theta}=\hat{\boldsymbol{\theta}}_{\text{ML}}} + \dots \quad (38)$$

The Laplace approximation takes advantage of the fact that when  $n$  is sufficiently large, the integrand is concentrated in a neighborhood of the mode of  $\hat{L}(\boldsymbol{\theta})$ , i.e., the maximum likelihood (ML) estimator  $\hat{\boldsymbol{\theta}}_{\text{ML}}$ . Thus,

$$\begin{aligned} m(\mathbf{z}^n) &= \int \exp\{\hat{L}(\boldsymbol{\theta})\} \pi(\boldsymbol{\theta}) d\boldsymbol{\theta} \\ &\approx \int \exp\left\{\hat{L}(\hat{\boldsymbol{\theta}}_{\text{ML}}) - \frac{n}{2}(\boldsymbol{\theta} - \hat{\boldsymbol{\theta}}_{\text{ML}})^\top J(\hat{\boldsymbol{\theta}}_{\text{ML}})(\boldsymbol{\theta} - \hat{\boldsymbol{\theta}}_{\text{ML}})\right\} \left(\pi(\hat{\boldsymbol{\theta}}_{\text{ML}}) + (\boldsymbol{\theta} - \hat{\boldsymbol{\theta}}_{\text{ML}})^\top \nabla \pi(\boldsymbol{\theta})|_{\boldsymbol{\theta}=\hat{\boldsymbol{\theta}}_{\text{ML}}}\right) d\boldsymbol{\theta} \\ &\stackrel{(a)}{\approx} \exp\{\hat{L}(\hat{\boldsymbol{\theta}}_{\text{ML}})\} \pi(\hat{\boldsymbol{\theta}}_{\text{ML}}) \int \exp\left\{-\frac{n}{2}(\boldsymbol{\theta} - \hat{\boldsymbol{\theta}}_{\text{ML}})^\top J(\hat{\boldsymbol{\theta}}_{\text{ML}})(\boldsymbol{\theta} - \hat{\boldsymbol{\theta}}_{\text{ML}})\right\} d\boldsymbol{\theta} \\ &= \exp\{\hat{L}(\hat{\boldsymbol{\theta}}_{\text{ML}})\} \pi(\hat{\boldsymbol{\theta}}_{\text{ML}}) (2\pi)^{p/2} n^{-p/2} |J(\hat{\boldsymbol{\theta}}_{\text{ML}})|^{-1/2}, \end{aligned}$$

where (a) follows from the following fact

$$\int (\boldsymbol{\theta} - \hat{\boldsymbol{\theta}}_{\text{ML}})^\top \exp\left\{-\frac{n}{2}(\boldsymbol{\theta} - \hat{\boldsymbol{\theta}}_{\text{ML}})^\top J(\hat{\boldsymbol{\theta}}_{\text{ML}})(\boldsymbol{\theta} - \hat{\boldsymbol{\theta}}_{\text{ML}})\right\} d\boldsymbol{\theta} = 0. \quad (39)$$

Taking the logarithm of this expression and multiplying it by  $-\frac{1}{n}$ , we obtain

$$-\frac{1}{n} \log(m(\mathbf{z}^n)) \approx -\frac{1}{n} \hat{L}(\hat{\boldsymbol{\theta}}_{\text{ML}}) + \frac{p}{2n} \log \frac{n}{2\pi} + \frac{1}{n} \log |J(\hat{\boldsymbol{\theta}}_{\text{ML}})| - \frac{1}{n} \log \pi(\hat{\boldsymbol{\theta}}_{\text{ML}}). \quad (40)$$

Note that  $J(\hat{\boldsymbol{\theta}}_{\text{ML}})$  is a random Hessian matrix. As  $n \rightarrow \infty$ ,  $J(\hat{\boldsymbol{\theta}}_{\text{ML}})$  will converge to its expectation by the consistency of MLE and the strong law of large numbers. Thus, both  $\log |J(\hat{\boldsymbol{\theta}}_{\text{ML}})|$  and  $\log \pi(\hat{\boldsymbol{\theta}}_{\text{ML}})$  have order less than  $O(1)$  with respect to the sample size  $n$ , and can be ignored in the BIC, which gives the following classical form of BIC:

$$\text{BIC} = -\frac{\hat{L}(\hat{\boldsymbol{\theta}}_{\text{ML}})}{n} + \frac{p \log n}{2n}. \quad (41)$$

## C Details of SGLD and Gibbs Algrotihm

In [35], it is shown that the following SGLD updates

$$\hat{W}_{t+1} = \hat{W}_t - \eta \nabla F_Z(W) + \sqrt{\frac{2\eta}{\beta}} \zeta_t, \quad t = 0, 1, \dots, \quad (42)$$

will converge to the Gibbs algorithm satisfying  $P_{\hat{W}|S} \propto \exp(-\beta F_Z(\hat{W}))$ . Note that our Gibbs algorithm contains an arbitrary prior distribution  $\pi$ , i.e.,  $P_{\hat{W}|S} \propto \pi(\hat{W}) \exp^{-nL_E(\hat{W}, S)}$ . To have the same format as  $F_Z(W)$ , we let

$$F_Z(w) = L_E(w, s) - \frac{1}{n} \log \pi(w). \quad (43)$$

Thus, the loss function used in the SGLD update becomes

$$\ell(w, z_i) = -\log P(y_i|x_i, w) - \frac{1}{n} \log \pi(w). \quad (44)$$

When the prior follows a Gaussian distribution  $\pi(w) \sim \mathcal{N}(0, \frac{\sigma^2}{\lambda n} I_p)$ , the second term in the loss function can be viewed as a regularization term derived from the log prior. It is crucial to notice that the empirical log loss in the subsequent SGLD computation only includes the  $L_E(w, s)$  term and does not incorporate the regularization term. As shown in [35], the regularizer term does not violate the assumptions used in the loss function, ensuring that our loss function will also converge to the desired Gibbs distribution.

## D Proof of Theorem 1

We note that the original idea of this result is coming from the discussion in Section 4 of [5].

We further assume that the parametric family  $\{P(z|\mathbf{w}), \mathbf{w} \in \mathcal{W}\}$  and prior  $\pi(\mathbf{w})$  satisfy all the regularization conditions required for the Bernstein–von-Mises theorem [42] and the asymptotic Normality of the maximum likelihood estimate (MLE), including Assumption 1 and the condition that  $\pi$  is continuous and  $\pi > 0$  for all  $\mathbf{w} \in \mathcal{W}$ .

For the Gibbs algorithm  $P_{\hat{W}|S}^*$  defined in (10), if we adopt the log-loss function  $\ell(w, \mathbf{z}) = -\log P(y|\mathbf{x}; w)$ , and set  $\beta = n$ , the Gibbs algorithm directly corresponds to the Bayesian posterior of the parametric family with prior distribution  $\pi$ . Therefore, in the asymptotic regime where  $p$  is fixed and  $n \rightarrow \infty$ , Bernstein–von-Mises theorem under model mismatch [42, 43] states that we could approximate the Gibbs algorithm in (10) by

$$\mathcal{N}(\hat{W}_{\text{ML}}, \frac{1}{n} J(\mathbf{w}^*)^{-1}),$$

with  $\mathbf{w}^*$  and  $J(\mathbf{w})$  defined in a similar manner as in (30). As  $n \rightarrow \infty$ , the asymptotic Normality of the MLE states that the distribution of  $\hat{W}_{\text{ML}}$  will converge to

$$\mathcal{N}(\mathbf{w}^*, \frac{1}{n} J(\mathbf{w}^*)^{-1} I(\mathbf{w}^*) J(\mathbf{w}^*)^{-1}).$$

Thus, the Gibbs distribution  $P_{\hat{W}|S}^*$  can be approximated as a Gaussian channel regardless of the choice of prior  $\pi(\mathbf{w})$ . Then, the symmetrized KL information can be computed using [44, Theorem 14], which characterizes the symmetrized KL information over a vector Gaussian channel, i.e.,

$$\frac{I_{\text{SKL}}(P_{\hat{W}|S}^*, P_S)}{n} = \frac{\text{tr}(I(\mathbf{w}^*) J(\mathbf{w}^*)^{-1})}{n} = \mathcal{O}\left(\frac{p}{n}\right). \quad (45)$$

Therefore, for the Gibbs algorithm  $P_{\hat{W}|S}^*$  defined in (10), if we adopt the log-loss function  $\ell(w, \mathbf{z}) = -\log P(y|\mathbf{x}; w)$ , and set  $\beta = n$ , and let  $n \rightarrow \infty$  with fixed  $p$ , we can get the following asymptotic expression for the generalization error,

$$\frac{I_{\text{SKL}}(P_{\hat{W}|S}^*, P_S)}{\beta} \rightarrow \frac{p}{n}. \quad (46)$$

Plug this result back to (14), the SGLD-based AIC can be written as,

$$\text{AIC}^+ = L_E(\hat{W}_{\text{SGLD}}, \mathbf{z}^n) + \frac{p}{n}. \quad (47)$$

## E Proof of Proposition 2

If we adopt the log-loss function  $\ell(w, z) = -\log P(y|\mathbf{x}; w)$ , and set  $\beta = n$ , the Gibbs distribution in (10) can be viewed as the Bayesian posterior distribution, i.e.,

$$P_{\hat{W}|S}^*(\mathbf{w}|\mathbf{z}^n) = \frac{\pi(\mathbf{w}) \prod_{i=1}^n P(y_i|\mathbf{x}_i; \mathbf{w})}{V(\mathbf{z}^n)}, \text{ with } V(\mathbf{z}^n) = \int \pi(\mathbf{w}) \prod_{i=1}^n P(y_i|\mathbf{x}_i; \mathbf{w}) d\mathbf{w}. \quad (48)$$

Therefore,

$$\begin{aligned} & \mathbb{E}_{P_{\hat{W}|S}^*} [L_E(\hat{W}, \mathbf{z}^n)] + \frac{1}{n} D(P_{\hat{W}|S}^* \|\pi) \\ &= \mathbb{E}_{P_{\hat{W}|S}^*} [L_E(\hat{W}, \mathbf{z}^n)] + \frac{1}{n} \mathbb{E}_{P_{\hat{W}|S}^*} \left[ \log \frac{\exp(-nL_E(\hat{W}, \mathbf{z}^n))}{V(\mathbf{z}^n)} \right] \\ &= -\frac{1}{n} \log V(\mathbf{z}^n) \\ &= -\frac{1}{n} \log m(\mathbf{z}^n), \end{aligned} \quad (49)$$

which completes the proof.

## F Proof of Theorem 2

Recall the SGLD-based BIC is given by

$$\text{BIC}^+ \triangleq L_E(\hat{W}_{\text{SGLD}}, \mathbf{z}^n) + \frac{1}{n} D(P_{\hat{W}|S}^* \|\pi). \quad (50)$$

Thus, we just need to characterize the asymptotic behavior of the KL divergence term in the regime where  $p$  is fixed and  $n \rightarrow \infty$ . Note that The KL divergence can be written as

$$\frac{1}{n} D(P_{\hat{W}|S}^* \|\pi) = -\frac{1}{n} H(P_{\hat{W}|S}^*) - \frac{1}{n} \mathbb{E}_{P_{\hat{W}|S}^*} [\log \pi(\hat{W})], \quad (51)$$

and  $P_{\hat{W}|S}^*$  will converge to  $\mathcal{N}(\hat{W}_{\text{ML}}, \frac{1}{n} J(\mathbf{w}^*)^{-1})$  by Bernstein–von-Mises theorem as shown in Appendix D. Then, the second term above will reduce to  $\frac{1}{n} \log \pi(\hat{W}_{\text{ML}})$ , and converges to zero as  $n \rightarrow \infty$ . Using the same Gaussian approximation, the entropy term can be computed as

$$H(P_{\hat{W}|S}^*) = \frac{p}{2} \log\left(\frac{2\pi e}{n}\right) + \frac{1}{2} \log |J(\mathbf{w}^*)^{-1}|. \quad (52)$$

As the number of samples  $n \rightarrow \infty$ ,  $\hat{W}_{\text{SGLD}} \rightarrow \hat{w}_{\text{ML}}$ . Therefore, the SGLD BIC can be asymptotically approximated by

$$\text{BIC}^+ = L_E(\hat{W}_{\text{SGLD}}, s) + \frac{1}{n} D(P_{\hat{W}|S}^* \|\pi) \quad (53)$$

$$= L_E(\hat{W}_{\text{SGLD}}, s) - \frac{1}{n} H(P_{\hat{W}|S}^*) - \frac{1}{n} \mathbb{E}_{P_{\hat{W}|S}^*} [\log \pi(\hat{W})] \quad (54)$$

$$= L_E(\hat{w}_{\text{ML}}, s) + \frac{p}{2n} \log \frac{n}{2\pi e} + \frac{1}{2n} \log |J(\mathbf{w}^*)| - \frac{1}{n} \log \pi(\hat{W}_{\text{ML}}). \quad (55)$$

Thus, both the terms  $p \log 2\pi e$ ,  $\log |J(\mathbf{w}^*)|$  and  $\log \pi(\hat{W}_{\text{ML}})$  have order less than  $O(1)$  with respect to the sample size  $n$ , and can be ignored in the SGLD-based BIC.

Comparing the above result with the log-marginal likelihood in (40), the penalty term in  $\text{BIC}^+$  differs from the classic BIC by  $\frac{p}{2n} \log e$ . This is due to the fact that we evaluate the same marginal likelihood  $m(\mathbf{z}^n)$  using different algorithms, and the empirical risk achieved by SGLD is different from that of the SGD.

## G Gibbs Distribution of Random Feature Model

For random feature model with the prior distribution  $\pi(w) \sim \mathcal{N}(0, \frac{\sigma^2}{\lambda n} \mathbf{I}_p)$  and  $L_E(w, s) = \frac{1}{n} \sum_{i=1}^n \log(y_i | x_i, w)$ , the log-posterior  $\log(P_{\hat{W}|S}^*) \propto \log \pi(w) + \log(e^{-nL_E(S)})$ , where

$$L_E(S) = \frac{1}{2n\sigma^2} \|\mathbf{Y} - \mathbf{B}\mathbf{w}\|_2^2 + \frac{1}{2} \log(2\pi\sigma^2).$$

Thus, the Gibbs algorithm, in this case, is given by the following Gaussian posterior distribution, as shown in [45],

$$P_{\hat{W}|S}^* \sim \mathcal{N}(\hat{W}_\lambda, \Sigma_w), \quad (56)$$

where  $\hat{W}_\lambda = (\lambda n \mathbf{I}_p + \mathbf{B}^\top \mathbf{B})^{-1} \mathbf{B}^\top \mathbf{Y}$ , and  $\Sigma_w = \sigma^2 (\lambda n \mathbf{I}_p + \mathbf{B}^\top \mathbf{B})^{-1}$ .

## H Proof of Theorem 3

We note that the KL divergence between two Gaussian distributions can be written as

$$D(\mathcal{N}(\boldsymbol{\mu}_1, \Sigma_1) \| \mathcal{N}(\boldsymbol{\mu}_2, \Sigma_2)) = \frac{1}{2} \left[ (\boldsymbol{\mu}_2 - \boldsymbol{\mu}_1)^\top \Sigma_2^{-1} (\boldsymbol{\mu}_2 - \boldsymbol{\mu}_1) + \text{tr}(\Sigma_2^{-1} \Sigma_1) - p + \log \frac{\det \Sigma_2}{\det \Sigma_1} \right].$$

The KL divergence between the Gibbs posterior of the RF model and the prior can be computed by,

$$\begin{aligned} \frac{1}{n} D(P_{\hat{W}|S=z^n}^* \| \pi) &= \frac{1}{2n} \left[ \hat{W}_\lambda^\top \left( \frac{\sigma^2}{\lambda n} \mathbf{I}_p \right)^{-1} \hat{W}_\lambda + \text{tr} \left( \frac{\lambda n}{\sigma^2} \Sigma_w \right) + \log \frac{\det \left( \frac{\sigma^2}{\lambda n} \mathbf{I}_p \right)}{\det(\Sigma_w)} - p \right] \\ &= \frac{1}{2n} \left[ \frac{\lambda n}{\sigma^2} \|\hat{W}_\lambda\|_2^2 + \text{tr} \left( \left( \mathbf{I}_p + \frac{\mathbf{B}^\top \mathbf{B}}{\lambda n} \right)^{-1} \right) + \log \det \left( \mathbf{I}_p + \frac{\mathbf{B}^\top \mathbf{B}}{\lambda n} \right) - p \right]. \end{aligned} \quad (57)$$

The trace and the log determinant of the random matrix  $\Sigma = \frac{\mathbf{B}^\top \mathbf{B}}{\lambda n} + \mathbf{I}_p$  can be computed using the following results from [38], which characterizes the probability density function of the eigenvalues of the random matrix  $\mathbf{B}^\top \mathbf{B}/n$  in the over-parameterized regime.

**Lemma 3.** [38] *Let the matrix  $\mathbf{M} = \frac{1}{n} \mathbf{B}^\top \mathbf{B} \in \mathbb{R}^{p \times p}$ , where  $\mathbf{B} = f\left(\frac{\mathbf{X}\mathbf{F}}{\sqrt{d}}\right) \in \mathbb{R}^{n \times p}$ , all the elements in  $\mathbf{F} \in \mathbb{R}^{d \times p}$  and  $\mathbf{X} \in \mathbb{R}^{n \times d}$  are generated i.i.d from  $\mathcal{N}(0, 1)$ . Suppose that the activation function has zero mean and finite moments, i.e.,*

$$\mathbb{E}[f(\varepsilon)] = 0, \quad \mathbb{E}[f(\varepsilon)^k] < \infty, \quad \text{for } k > 1, \quad \varepsilon \sim \mathcal{N}(0, 1). \quad (58)$$

and define constants  $\eta$  and  $\xi$  as

$$\eta \triangleq \mathbb{E}[f(\varepsilon)^2], \quad \xi \triangleq \mathbb{E}[f'(\varepsilon)]^2, \quad \varepsilon \sim \mathcal{N}(0, 1), \quad (59)$$

as  $n, d, p \rightarrow \infty$  with  $d/p \rightarrow \psi$ ,  $d/n \rightarrow \phi$ , where  $\psi, \phi \in (0, \infty)$ , then the Stieltjes transform  $G(z)$  of the spectral density of random matrix  $\mathbf{M}$  satisfies

$$dF_{\mathbf{M}}(x) = \frac{1}{\pi} \lim_{\epsilon \rightarrow 0^+} \text{Im} G(x - i\epsilon), \quad G(z) = \frac{\psi}{z} A\left(\frac{1}{z\psi}\right) + \frac{1-\psi}{z}, \quad (60)$$

$$A(t) = 1 + (\eta - \xi)t A_\phi(t) A_\psi(t) + \frac{A_\phi(t) A_\psi(t) t \xi}{1 - A_\phi(t) A_\psi(t) t \xi}, \quad (61)$$

where  $A_\phi(t) = 1 + (A(t) - 1)\phi$  and  $A_\psi(t) = 1 + (A(t) - 1)\psi$ .

This lemma characterizes the spectral density of random matrix  $\mathbf{M}$  for any zero-mean activation functions. However, these implicit equations need to be evaluated numerically, and it is hard to obtain a closed-form expression or provide more insights.

If we further assume that the assumptions in (23) are satisfied, i.e.,  $\mathbb{E}[f(\varepsilon)^2] = 1$ , and  $\mathbb{E}[f'(\varepsilon)]^2 = 0$ , then the result in Lemma 3 can be simplified significantly, as the probability density of the eigenvalues for random matrix  $\mathbf{M}$  will converge to the well-known Marchenko-Pastur distribution with shape parameter  $r = p/n$ , i.e.,

$$dF_{\mathbf{M}}(x) \rightarrow \left(1 - \frac{1}{r}\right)^+ \delta(x) + \frac{\sqrt{(x-a)^+(b-x)^+}}{2\pi r x}, \quad (62)$$

as  $n, d, p$  all go to infinity, where  $(z)^+ \triangleq \max\{0, z\}$ , and  $a \triangleq (1 - \sqrt{r})^2$ , and  $b \triangleq (1 + \sqrt{r})^2$ . Thus, we focus on this case to obtain a convenient, closed-form expression for mutual information.

The following lemma from Sections 2.2.2 and 2.2.3 in [39] characterizes the  $\eta$ -transform and Shannon transform of the Marchenko-Pastur distribution.

**Lemma 4.** *The  $\eta$  and Shannon transform of a nonnegative random variable  $X$  are defined as*

$$\eta_X(\gamma) \triangleq \mathbb{E}\left[\frac{1}{1 + \gamma X}\right], \quad \mathcal{V}_X(\gamma) \triangleq \mathbb{E}[\log(1 + \gamma X)], \quad (63)$$

respectively. If  $X$  is distributed according to Marchenko-Pastur distribution with shape parameter  $r = p/n$ , then

$$\eta_X(\gamma) = 1 - \frac{\mathcal{F}(\gamma, r)}{4r\gamma}, \quad (64)$$

$$\mathcal{V}_X(\gamma) = \log\left(1 + \gamma - \frac{1}{4}\mathcal{F}(\gamma, r)\right) + \frac{1}{r} \log\left(1 + \gamma r - \frac{1}{4}\mathcal{F}(\gamma, r)\right) - \frac{1}{4r\gamma}\mathcal{F}(\gamma, r), \quad (65)$$

where

$$\mathcal{F}(\gamma, r) \triangleq \left(\sqrt{\gamma(1 + \sqrt{r})^2 + 1} - \sqrt{\gamma(1 - \sqrt{r})^2 + 1}\right)^2. \quad (66)$$

Equipped with the aforementioned tools from random matrix theory, we could proceed our analysis,

$$\frac{1}{n} \log \det \left(\mathbf{I}_p + \frac{1}{\lambda n} \mathbf{B}^\top \mathbf{B}\right) = \frac{r}{p} \sum_{i=1}^p \log \left(1 + \frac{1}{\lambda} \lambda_i \left(\frac{1}{n} \mathbf{B}^\top \mathbf{B}\right)\right), \quad (67)$$

where the notation  $\lambda_i(\cdot)$  denote the eigenvalues of the matrix for  $i = 1, \dots, p$ . As shown in Lemma 4, we have

$$\frac{1}{p} \sum_{i=1}^p \log \left(1 + \frac{1}{\lambda} \lambda_i \left(\frac{1}{n} \mathbf{B}^\top \mathbf{B}\right)\right) \rightarrow \int_0^\infty \log \left(1 + \frac{x}{\lambda}\right) dF_M^n(x) = \mathcal{V}_X(1/\lambda) \quad (68)$$

almost surely, when  $n, d, p \rightarrow \infty, p/n = r$ . Thus, in the over-parameterized regime, we have

$$\frac{1}{n} \log \det \left(\mathbf{I}_p + \frac{1}{\lambda n} \mathbf{B}^\top \mathbf{B}\right) \rightarrow r \cdot \mathcal{V}_X(1/\lambda) = V(1/\lambda, r). \quad (69)$$

And the trace term can be simplified as,

$$\frac{1}{n} \text{tr} \left(\mathbf{I}_p + \frac{1}{\lambda n} \mathbf{B}^\top \mathbf{B}\right)^{-1} = r \frac{1}{p} \sum_{i=1}^p \frac{1}{\left(1 + \frac{1}{\lambda} \lambda_i \left(\frac{1}{n} \mathbf{B}^\top \mathbf{B}\right)\right)}, \quad (70)$$

which will converge to the following expression by Lemma 4, when  $n, d, p \rightarrow \infty, p/n = r$ ,

$$r \frac{1}{p} \sum_{i=1}^p \frac{1}{\left(1 + \frac{1}{\lambda} \lambda_i \left(\frac{1}{n} \mathbf{B}^\top \mathbf{B}\right)\right)} \rightarrow r \int_0^\infty \frac{1}{1 + \frac{x}{\lambda}} dF_M^n(x) = r \left(1 - \frac{\mathcal{F}(\frac{1}{\lambda}, r)}{4r \frac{1}{\lambda}}\right). \quad (71)$$

Combine (69) and (71) with (57), we obtain the following result

$$\frac{1}{n} D(P_{\hat{W}|S=z^n}^* \|\pi) \rightarrow \frac{\lambda}{2\sigma^2} \|\hat{W}_\lambda\|_2^2 - \frac{\lambda}{8} \mathcal{F}\left(\frac{1}{\lambda}, r\right) + \frac{1}{2} V(1/\lambda, r). \quad (72)$$

## H.1 Empirical Behavior of Covariance Term

To show that Theorem 3 can provide a good approximation for the asymptotic behavior of the log determinant and trace term in (22), we plot in Figure 5 both the term  $1/n(\log |\Sigma| + \text{tr}(\Sigma)^{-1} - p)$  with finite data and  $\frac{1}{2}V(1/\lambda, r) - \frac{\lambda}{8}\mathcal{F}(\frac{1}{\lambda}, r)$  in the over-parameterized SGLD-based BIC for different activation functions with varying regularizer parameters  $\lambda$ . As shown from Figure 5(left), our theoretical results provide a good proxy for the asymptotic behavior of the covariance term, even for activation functions (e.g., ReLU and Sigmoid in Figure 5(middle and right)) that do not satisfy the assumptions in Theorem 3. This is evidence that the particular choice of activation function does not significantly influence the asymptotic behavior of the covariance term in SGLD-based BIC.

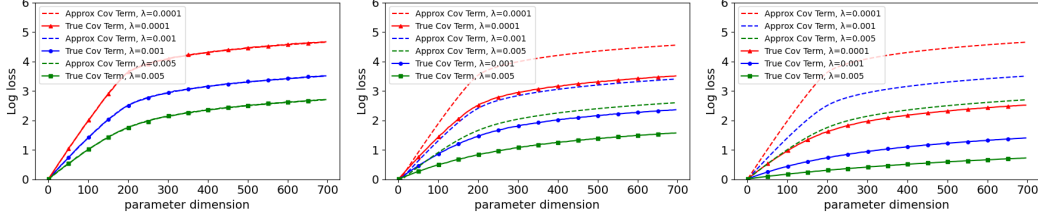


Figure 5: A comparison between  $1/n(\log|\Sigma| + \text{tr}(\Sigma)^{-1} - p)$  and the asymptotic approximation of the covariance term in Theorem 3 for different value of  $\lambda$  and for different activation functions:  $f(x) = (x^2 - 1)/\sqrt{2}$  (left), ReLU (middle) and Sigmoid (right). We adopt the same experiment settings as in Section 5.2, and we change  $r = p/n$  by fixing  $n = 200$  and varying  $p$ .

## I Additional Experimental Results

We present additional comparison plots for different values of  $\lambda$  in Figure 6 and 7. These figures correspond to the experimental setting described in Section 5, illustrating the mismatch between the generalization error and KL divergence. Moreover, it is evident from these figures that with different parameter settings, different terms will dominate the KL divergence in the SGLD-based BIC.

### I.1 Experimental Details

In our experiments, the setup for the random feature model is akin to a two-layer neural network with a ReLU activation function. The first layer is initialized with a Gaussian distribution  $\mathcal{N}(0, \frac{1}{\sqrt{d}})$  and remains unchanged throughout the training. The second layer, which starts off with zero values, is trained using the log loss function.

We set the step size for both SGD and SGLD to 0.01. The training process typically converges around 100 epochs. However, to ensure convergence to the Gibbs distribution, we continue to run SGLD for a substantial number of epochs (400 in our experiment) even after achieving the minimum training loss. In addition, although we trained the noise variance in the classic regime to calibrate it to an appropriate scale, we fixed the noise variance  $\sigma^2$  to 0.81 due to the high variability in model complexity in the over-parameterized regime.

Our experiments, implemented in PyTorch requires less than 24 hours of training computation time on a single RTX 3090 GPU. To ensure result accuracy and plot error bars, we perform 50 runs for each setting.

### I.2 RF model loss

Keeping remind that the following loss function is only used in SGLD training process,

$$\mathcal{L}(\mathbf{w}) = - \sum_{i=1}^n \left( \log P(y_i|x_i, \mathbf{w}) - \frac{1}{n} \log \pi(\mathbf{w}) \right) \quad (73)$$

$$= \frac{1}{2\sigma^2} \sum_{i=1}^n \left( y_i - f \left( \frac{\mathbf{x}_i^\top \mathbf{F}}{\sqrt{d}} \right) \mathbf{w} \right)^2 + \frac{n}{2} \log(2\pi\sigma^2) + \frac{\lambda n \|\mathbf{w}\|_2^2}{2\sigma^2}. \quad (74)$$

For traditional AIC and BIC, we optimize the following log-likelihood using SGD,

$$\mathcal{L}(\mathbf{w}) = \frac{1}{2\sigma^2} \sum_{i=1}^n \left( y_i - f \left( \frac{\mathbf{x}_i^\top \mathbf{F}}{\sqrt{d}} \right) \mathbf{w} \right)^2 + \frac{n}{2} \log(2\pi\sigma^2). \quad (75)$$

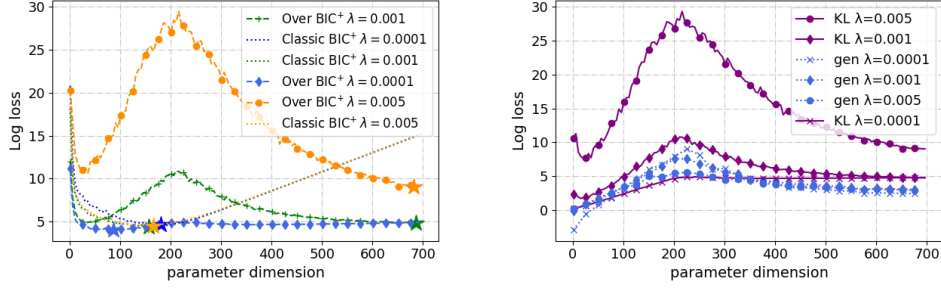


Figure 6: A comparison of  $BIC^+$  in the over-parameterized and classical regime with all  $\lambda$  in the Experiment (**left**). A comparison between the KL divergence term in  $BIC^+$  and the generalization error term in  $AIC^+$  with with all  $\lambda$  in the Experiment (**right**).

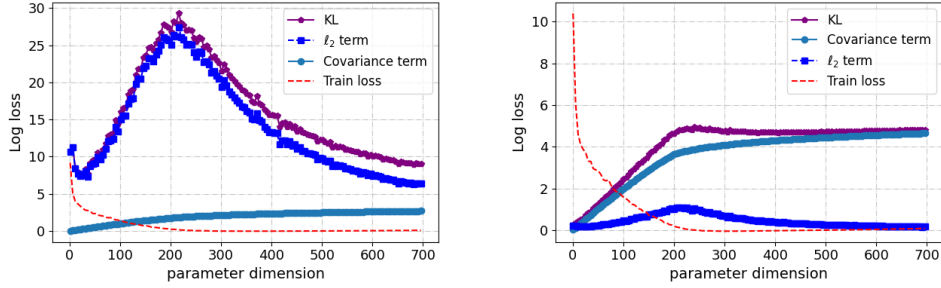


Figure 7: A decomposition of the four terms in over-parameterized  $BIC^+$  in (27) with  $\lambda = 0.005$  (**left**) and  $\lambda = 0.0001$  (**right**)

### I.3 Real Data

We have the following representative experimental results involving a Relative location of CT slices on axial axis dataset from UCI Machine Learning repository<sup>1</sup>. The task is extracted from CT images. The class variable  $X \in \mathbb{R}^{384}$  is numeric and denotes the relative location  $Y$  of the CT slice on the axial axis of the human body. We split the data into train ( $n = 180$ ) and test (120 samples) sets and set the  $\lambda = 0.00005$  and  $\sigma^2 = 0.25$  run for 800 epochs. For the other parameters and RF model setup, we adopt the same settings as in the previous experiment in Section 5.2. The results are shown in Figure 8.

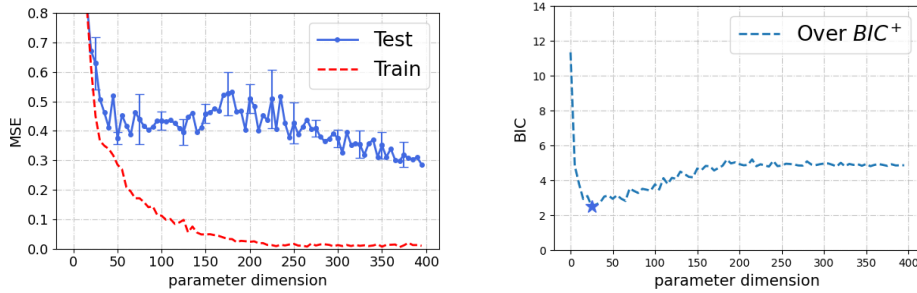


Figure 8: Train/Test MSE and the SGLD  $BIC^+$  with Relative location of CT slices on axial axis dataset

<sup>1</sup><https://archive.ics.uci.edu/ml/datasets/Relative+location+of+CT+slices+on+axial+axis>